Coding for Two-Head Recording Systems

Emina Soljanin and Costas N. Georghiades, *Senior Member, IEEE*

***Abstract*— A reduction in the track width in disc-recording systems results in a desirable increase in areal density, but also in the undesirable appearance of inter-track interference (ITI) and loss of signal-to-noise ratio (SNR). One way the effects of ITI may be alleviated is through the use of multiple-head systems simultaneously writing and reading a number of adjacent tracks. In this paper we investigate the performance of two-track detectors, and design codes that combat two-dimensional interference patterns, ISI in the axial dimension, and ITI in the radial dimension, and recover the loss in SNR due to track-narrowing. Sliding-block decoders and reduced-complexity Viterbi detectors are also designed for these codes, which are seen to more than compensate for the performance loss for a large range of ITI levels.**

***Index Terms*—Recording systems, intertrack-interference, coding, multi-track multi-head systems, MSN codes.**

I. Introduction

EVEN THOUGH already a multi-billion dollar industry, the digital recording industry is expected to expand further in the future as an almost insatiable appetite for more storage continuous to grow. This increase is partly fueled by the steady move towards digital systems, as has happened, for example, in the audio industry with the replacement of the analog long-play (LP) record by the digital compact disc (CD). Digital disc recording systems include magnetic and optical recording. Whether optical or magnetic, one of the main goals of ongoing research is to increase areal density in bits per unit area.

One way areal density can be increased along the radial direction is by narrowing the track width, thus allowing more tracks per unit radial distance (see Siegel and Wolf [1]). As a result of the track narrowing, however, there is a loss in signal-to-noise ratio (SNR) during readback, as well as increased intertrack interference (ITI). The loss in SNR can be compensated for by employing a code that improves noise immunity in each track, which in turn decreases in-track density. A potential areal density gain can be obtained provided high-rate codes that can combat both ISI and ITI and make up for the SNR loss can be designed. For example, if track width decreases by a factor of two, SNR drops by 3 dB, based on the assumption that the amplitude of the readback signal and the power of the noise due to the medium reduce approximately by a factor of two (see Siegel and Wolf [1] and the references therein). Applying a code that provides a 3-dB gain at a rate higher than 1/2 will achieve an overall density increase compared to the original, uncoded system, for the same performance. The new code, however, should provide the required gain for a wide range of ITI values since track narrowing increases ITI.

It has been acknowledged that inter-track interference is an important noise source in disc recording systems, whose effects can be significantly reduced by means of multiple recording heads (see Barbosa [2]–[4], Abbot, Cioffi, and Thapar [5], and Voois and Cioffi [6]–[8]). An additional benefit of writing and reading multiple tracks in parallel is that information for timing and gain control can be obtained from *any* track, which was shown by Marcellin and Weber [9] and Swanson and Wolf [10] to reduce the required redundancy and enable substantial increases in areal density. All this suggests that simultaneous detection of readback signals from interfering tracks using array heads be further investigated as a means of increasing areal density in disc recording systems.

Although the use of multiple heads with simultaneous detection can reduce the effects of ITI on performance, there is nevertheless a residual performance loss incurred by track narrowing. This performance loss can be recovered by the use of coding, which as we will see later in the paper, can not only compensate for the loss, but also provide some extra gain. In general, the code must be designed to account for a two-dimensional interference pattern, ISI in the axial dimension and ITI in the radial direction. It has been shown in [11], [12] that for a range of low ITI levels, existing codes (such as the matched spectral null (MSN) codes studied by Karabed and Siegel [13]) designed for single-track, single-head systems, applied uncooperatively on each track can enhance error rate performance for multi-head, multi-track systems. However, independently coding each track using existing codes fails to provide adequate coding gains when ITI exceeds a certain threshold.

In this paper we design modulation codes capable of combating the performance loss due to inter-track interference caused by track narrowing in two-track, two-head systems. The designed codes, which achieve coding gains for a wide range of ITI values, are at high enough rates to provide an overall areal density increase, and satisfy run-length constraints that facilitate timing and gain recovery. The finite state diagrams (FSTD's) for the two-dimensional codes are derived as subgraphs of the graph representing the cross-product of two FSTD's corresponding to single-track MSN codes. Like the latter, the two-dimensional codes provide high rate, noise

Manuscript received December 9, 1993; revised October 17, 1994. This work was supported by the National Science Foundation under Grant NCR-9016329. The material in this paper was presented at the IEEE International Symposium on Information Theory, Trondheim, Norway, June 1994.

E. Soljanin was with the Electrical Engineering Department, Texas A&M University, College Station, TX 77843-3128 USA. She is now with AT&T Bell Laboratories, Murray Hill, NJ 07974 USA.

C. N. Georghiades is with the Electrical Engineering Department, Texas A&M University, College Station, TX 77843-3128 USA.

IEEE Log Number 9410418.

0018–9448/95$04.00 © 1995 IEEE

immunity, satisfy run-length constraints, and have sliding-block decoders and reduced complexity Viterbi detectors.

In Section II we present a simple model for the multi-track, multi-head digital recording channel, the log-likelihood function, and a lower bound on the error probability. In Section III, we discuss the special case of two-track, two-head systems, present a class of FSTD's for two-track codes, and analyze their distance properties. We then construct several codes from these FSTD's and test their performance by simulation. Finally, Section IV contains our conclusions.

II. Systems with Intertrack Interference

This section summarizes the results of [11], [12] on multi-track, multi-head systems, necessary for discussing coding in two-track, two-head systems. A simple, linear channel model that accounts for intertrack interference in multiple-head systems is described next. Even though quite simplified, we hope that the model captures the essential effects of ITI present in the real channel. We assume that there are no servo positioning errors, but the designed codes could be applied to the case when such errors are present as well.

A. Channel Model

Sequences of L-dimensional vectors

$$\overline{a}_n = (a_{n1}, a_{n2}, \cdots, a_{nL}) \in \{-1, 1\}^L$$

are written on the medium in L adjacent tracks. There are K reading heads flying over these tracks simultaneously reading each. The kth, $k = 1, \cdots, K$, head responds to the magnetization of the lth, $l = 1, \cdots, L$, track by producing a signal as if it were positioned over that track, but with an amplitude modified by a weighting parameter α_{kl}. We let

$$\mathcal{A} = \{\overline{\alpha}_k = (\alpha_{k1}, \alpha_{k2}, \cdots, \alpha_{kL})\}_{k=1}^K$$

be the $K \times L$ matrix containing the ITI parameters. In saturation recording, the total read-head response is the superposition of responses to individual flux reversals, which makes the reading process essentially linear. We assume that the noise in the system is additive, white, and Gaussian due to the electronics on the read side and the medium (in reality, the noise component due to the medium is colored). Thus the signal read by the kth head is

$$r_k(t) = \sum_{l=1}^{L} \alpha_{kl} \left(\sqrt{E} \sum_{n=-\infty}^{\infty} a_{nl} h(t - nT) \right) + w_k(t), \qquad 1 \le k \le K \quad (1)$$

where $h(t)$ is a unit-energy pulse and $w_k(t)$ are independent, white, Gaussian random processes having zero mean and power spectral density σ^2. We refer to E/σ^2 as the *signal-to-noise ratio* (SNR) *per track*. The multi-track detector observes the K signals and uses them to produce maximum-likelihood sequence estimates (MLSE) of the recorded data.

B. Optimal Multi-Track Detection

Assuming $\boldsymbol{a} = \{\overline{a}_n\}_{n=-\infty}^{\infty}$ and $\boldsymbol{w} = \{w_k(t)\}_{k=1}^K$ are stochastically independent, it can be shown [12] that the optimum detector (maximum-likelihood sequence estimator) for a recording channel with L tracks and K heads chooses an allowable sequence $\hat{\boldsymbol{a}}$ that maximizes the log-likelihood function

$$\Omega(\boldsymbol{a}) = \sum_{n=-\infty}^{\infty} \overline{a}_n \mathcal{A}' \overline{y}_n' - \frac{\sqrt{E}}{2} \cdot \sum_{n=-\infty}^{\infty} \sum_{m=-\infty}^{\infty} \overline{a}_n \mathcal{A}' \mathcal{A} \overline{a}_m' x_{n-m} \quad (2)$$

where primes indicate transapose,

$$\overline{y}_n = (y_{n1}, y_{n2}, \cdots, y_{nK})$$
$$y_{nk} = \int_{-\infty}^{\infty} h(t - nT) r_k(t)\, dt, \qquad 1 \le k \le K \quad (3)$$

and

$$x_n = \int_{-\infty}^{\infty} h(t) h(t - nT)\, dt. \quad (4)$$

Note that

$$\{x_k\} \overset{\text{DFT}}{\longleftrightarrow} X(D) = F(D) F^*(D^{-1})$$

where $F(D)$ is usually modeled as

$$F(D) = g(1 - D)(1 + D)^n$$

($g > 0$ is a normalizing constant).

C. Error Probability Performance

Let $\boldsymbol{a} = \{\overline{a}_n\}_{n=-\infty}^{\infty}$ and $\boldsymbol{b} = \{\overline{b}_n\}_{n=-\infty}^{\infty}$ be two allowable recorded sequences and $\boldsymbol{\epsilon} = (\boldsymbol{a} - \boldsymbol{b})/2$ be the normalized error sequence corresponding to $\boldsymbol{a}$ and $\boldsymbol{b}$. Then the distance between $\boldsymbol{a}$ and $\boldsymbol{b}$ is

$$d^2(\boldsymbol{\epsilon}) = \sum_{n=-\infty}^{\infty} \sum_{m=-\infty}^{\infty} \overline{\epsilon}_n \mathcal{A}' \mathcal{A} \overline{\epsilon}_m' x_{n-m}. \quad (5)$$

The lower bound to the minimum probability of an error event in the system is proportional to $Q(d_{\min} \cdot \sqrt{\text{SNR}})$, where

$$d_{\min}^2 = \min_{\boldsymbol{\epsilon} \neq \boldsymbol{0}} d^2(\boldsymbol{\epsilon})$$

and $\boldsymbol{\epsilon}$ has only a finite number of nonzero elements.

To examine the minimum distance properties of the two-track, two-head systems discussed in the next section, we derive another form of (5) for $d^2(\boldsymbol{\epsilon})$. For the most common models of interference $\mathcal{A}'\mathcal{A}$ is Toeplitz and symmetric, i.e., $\mathcal{A}'\mathcal{A} = \{\gamma_{lj}\}_{L \times L}$, where $\gamma_{li} = \gamma_{il} = s_{|l-i|}$. A normalized error sequence $\boldsymbol{\epsilon}$ is a sequence of normalized error vectors $\overline{\epsilon}_n \in \{-1, 0, 1\}^L$ whose nonzero entries indicate the positions of bit-errors in the L tracks at time $n, -\infty \le n \le \infty$. It can also be represented as a vector of normalized error sequences $\overline{e}_l \in \mathcal{E}_t^l$ with nonzero entries indicating the position of bit-errors in the lth track, $1 \le l \le L$, for all $n, -\infty \le n \le \infty$, i.e.

$$\boldsymbol{\epsilon} = \{\overline{e}_l \in \mathcal{E}_t^l\}_{l=1}^L$$

where $\mathcal{E}_t^l$ is equal to the set $\{-1,0,1\}^\infty$ for uncoded systems, or is a subset of it for coded systems. Thus the above expression for $d^2(\epsilon)$ can be rewritten as

$$d^2(\epsilon) = \sum_{l=1}^{L}\sum_{i=1}^{L} \overline{e}_l X \overline{e}_i' s_{|l-i|} \tag{6}$$

where $X = \{\chi_{nm}\}$ is a matrix with elements

$$\chi_{nm} = x_{n-m}, \quad -\infty \le n, m \le \infty.$$

For X positive-definite, we can define an inner product in R^∞ as $\langle \overline{u}, \overline{v}\rangle_X = \overline{u}X\overline{v}', \overline{u}, \overline{v} \in R^\infty$. The norm of a vector $\overline{u} \in R^\infty$ is then $\|\overline{u}\|_X^2 = \langle \overline{u}, \overline{u}\rangle_X$, and by the Cauchy–Schwarz inequality $|\langle \overline{u}, \overline{v}\rangle_X|^2 \le \|\overline{u}\|_X^2 \cdot \|\overline{v}\|_X^2$. Note that X is positive-definite iff $F(D)$ is nonzero except over a set of measure zero, which is satisfied by the class of $F(D)$ commonly used to model magnetic recording channels.

In the next section we state and prove three propositions that are used to provide insight into the code design problem for multiple-head systems.

III. Coding for Two-Track, Two-Head Disc Recording Systems

A. Distance Properties of Uncoded Systems

In what follows, we consider the special case of systems with two interfering tracks simultaneously read by two heads. In this case

$$\mathcal{A} = \begin{bmatrix} 1 & \alpha \\ \alpha & 1 \end{bmatrix}. \tag{7}$$

We will first examine the distance properties of these systems. A special case of this problem when

$$\{x_k\} \overset{\text{DFT}}{\longleftrightarrow} X(D) = F(D)F^*(D^{-1})$$
$$F(D) = (1+D)/\sqrt{2}$$

was first considered by Barbosa in [4]. The following proposition formally proves the results of [4] and generalizes them for arbitrary $X(D)$. The statement of the proposition and its proof imply a corollary that gives insight into the coding problem for these systems.

Proposition 1: Let d_0 be a single-track minimum distance parameter defined by

$$d_0^2 = \min_{\overline{e}\in\mathcal{E}_t, \overline{e}\neq \mathbf{0}} \|\overline{e}\|_X^2 \tag{8}$$

where for the two-head, two-track case under consideration $\mathcal{E}_t = \mathcal{E}_t^1 = \mathcal{E}_t^2$. Then

$$d_{\min}^2 = \begin{cases} (1+\alpha^2)d_0^2, & \text{if } 0 \le \alpha \le 2-\sqrt{3} \\ 2(1-\alpha)^2 d_0^2, & \text{if } 2-\sqrt{3} \le \alpha \le 1/2. \end{cases} \tag{9}$$

Proof of Proposition 1: The minimum distance $d_{\min}^2$ is obtained by minimizing $d^2(\epsilon)$ defined in (6). For two-track, two-head systems $d^2(\epsilon)$ is given by

$$d^2(\epsilon) = (1+\alpha^2)(\|\overline{e}_1\|_X^2 + \|\overline{e}_2\|_X^2) + 2\cdot 2\alpha\langle \overline{e}_1, \overline{e}_2\rangle_X$$

with $\epsilon = (\overline{e}_1, \overline{e}_2), \overline{e}_1, \overline{e}_2 \in \mathcal{E}_t$. We partition the set of all possible error sequences ϵ into two subsets:

1) Error sequences containing only single-track errors, i.e., either $\overline{e}_1 = \overline{0}$ or $\overline{e}_2 = \overline{0}$, for which
$$\begin{aligned} d^2(\epsilon) &= (1+\alpha^2)(\|\overline{e}_1\|_X^2 + \|\overline{e}_2\|_X^2) \\ &\ge (1+\alpha^2)d_0^2. \end{aligned}$$
Equality is achieved when the nonzero error vector $\overline{e}_l$ satisfies $\|\overline{e}_l\|_X^2 = d_0^2$.
2) Error sequences with double-track errors, i.e., $\overline{e}_1 \neq \overline{0}$ and $\overline{e}_2 \neq \overline{0}$, for which
$$\begin{aligned} d^2(\epsilon) &= (1+\alpha^2)(\|\overline{e}_1\|_X^2 + \|\overline{e}_2\|_X^2) + 2\cdot 2\alpha\langle \overline{e}_1, \overline{e}_2\rangle_X \\ &\ge (1+\alpha^2)(\|\overline{e}_1\|_X^2 + \|\overline{e}_2\|_X^2) - 2\cdot 2\alpha|\langle \overline{e}_1, \overline{e}_2\rangle_X| \\ &\ge (1+\alpha^2)(\|\overline{e}_1\|_X^2 + \|\overline{e}_2\|_X^2) - 2\cdot 2\alpha\|\overline{e}_1\|_X \cdot \|\overline{e}_2\|_X \\ &\ge (1+\alpha^2)(\|\overline{e}_1\|_X^2 + \|\overline{e}_2\|_X^2) - 2\alpha(\|\overline{e}_1\|_X^2 + \|\overline{e}_2\|_X^2) \\ &= (1-\alpha)^2(\|\overline{e}_1\|_X^2 + \|\overline{e}_2\|_X^2) \\ &\ge 2(1-\alpha)^2 d_0^2. \end{aligned}$$
Equality is achieved when $\overline{e}_1 = -\overline{e}_2$ and $\|\overline{e}_1\|_X^2 = \|\overline{e}_2\|_X^2 = d_0^2$.

The minimum distance as a function of α is the minimum of the two distances, $(1+\alpha^2)d_0^2$ and $2(1-\alpha)^2 d_0^2$, giving

$$d_{\min}^2 = \begin{cases} (1+\alpha^2)d_0^2, & \text{if } (1+\alpha^2) < 2(1-\alpha)^2 \\ 2(1-\alpha)^2 d_0^2, & \text{if } (1+\alpha^2) \ge 2(1-\alpha)^2. \end{cases}$$

The above expression reduces to (9) in the proposition for $0 \le \alpha \le 1/2$. ■

Note that, because of multiple heads, there is no performance loss due to ITI as long as $d_{\min}^2 \ge d_0^2$, i.e., $0 \le \alpha \le \sqrt{2}/2$.

Corollary 1: A single-track code that provides an increase in the single-track minimum distance to $d_0^c = \sqrt{g}d_0$ when applied to each track, results in an increase in the two-track minimum distance to $d_{\min}^c = \sqrt{g}d_{\min}$.

Example 1: Consider a two-track, two-head system in which ITI is described by (7) and each track is modeled as a $(1-D)$ channel

$$\{x_k\} \overset{\text{DFT}}{\longleftrightarrow} X(D) = F(D)F^*(D^{-1}), \quad F(D) = (1-D)/\sqrt{2}.$$

The single-track minimum distance parameter for an uncoded system is $d_0^2 = 1$. Suppose that the SNR loss incurred by the system by track narrowing is 3 dB.

If the biphase code of rate 1/2, which provides an increase in single-track minimum distance to $d_0^c = \sqrt{3}d_0$, is applied to each track, then the two-track minimum distance will be

$$d_{\min}^2 = \begin{cases} 3(1+\alpha^2), & \text{if } 0 \le \alpha \le 2-\sqrt{3} \\ 6(1-\alpha)^2, & \text{if } 2-\sqrt{3} \le \alpha \le 1/2. \end{cases}$$

The SNR loss of 3 dB will be recovered for $d_{\min}^2 \ge 2$ or $0 \le \alpha \le 1-\sqrt{3}/3$. For $1-\sqrt{3}/3 \le \alpha \le 1/2$, there

is additional loss in performance due to ITI that cannot be recovered by the code.

If a matched-spectral-null code [13] of rate higher than 1/2 (which provides an increase in single-track minimum distance to $d_0^c = \sqrt{2}d_0$) is applied to each track, then the two-track minimum distance will be

$$d_{\min}^2 = \begin{cases} 2(1+\alpha^2), & \text{if } 0 \le \alpha \le 2-\sqrt{3} \\ 4(1-\alpha)^2, & \text{if } 2-\sqrt{3} \le \alpha \le 1/2. \end{cases}$$

The SNR loss of 3 dB will be recovered for $d_{\min}^2 \ge 2$ or $0 \le \alpha \le 1 - \sqrt{2}/2$. Clearly, if we apply higher rate codes, the range of interference levels for which the SNR loss can be recovered becomes smaller.

Therefore, codes designed for improving noise immunity in single-track systems can provide a coding gain in two-track, two-head systems. However, these codes are not capable of recovering the loss in performance due to ITI, since they are not designed to account for it.

B. Distance Properties of Two-Track Codes

We now introduce a class of two-dimensional codes capable of combating the SNR loss due to ITI for the two-track, two-head systems with ITI described by (7) and for the $(1 - D)$ channel. Matched-spectral-null (MSN) codes are high-rate single-track codes, which provide both run-length constraints required for timing and gain control and improved noise immunity. They have sliding-block decoders and reduced complexity suboptimal Viterbi detectors. Because of these properties, we derive a class of finite-state diagrams FSTD's for two-track codes from the graph representing the cross-product of two canonical diagrams of single-track MSN codes.

Definition 1: Let G be an irreducible FSTD whose vertices are labeled by L-dimensional symbols $\overline{u} = (u_1, u_2, \cdots, u_L) \in \{0,1\}^L$ corresponding to the bits in L tracks at some fixed time. Let $\boldsymbol{u} = \overline{u}_0, \cdots, \overline{u}_n$ and $\boldsymbol{v} = \overline{v}_0, \cdots, \overline{v}_n$ be sequences which are generated by paths in G starting at the same state.

- We refer to the sequence $\boldsymbol{\epsilon} = \overline{\epsilon}_0, \cdots, \overline{\epsilon}_n$, where

$$\begin{aligned} \overline{\epsilon}_i &= (\epsilon_{i1}, \epsilon_{i2}, \cdots, \epsilon_{iL}) \\ &= (u_{i1} - v_{i1}, u_{i2} - v_{i2}, \cdots, u_{iL} - v_{iL}) \end{aligned} \tag{10}$$

  as the *difference sequence* corresponding to $\boldsymbol{u}$ and $\boldsymbol{v}$.
- If the sequences $\boldsymbol{u}$ and $\boldsymbol{v}$ also end in the same state we call $\boldsymbol{\epsilon}$ a *difference event*, and if the starting and ending states coincide, $\boldsymbol{\epsilon}$ is a *difference cycle*.
- We refer to the sequence $\overline{e}_l = \epsilon_{0l}, \cdots, \epsilon_{nl}$ as the difference sequence corresponding to $\boldsymbol{u}$ and $\boldsymbol{v}$ on track l, $1 \le l \le L$.
- We refer to the polynomial

$$e_l(D) = \sum_{m=0}^{n} \epsilon_{ml} D^m$$

  as the *difference polynomial* corresponding to $\overline{e}_l, 1 \le l \le L$. ■

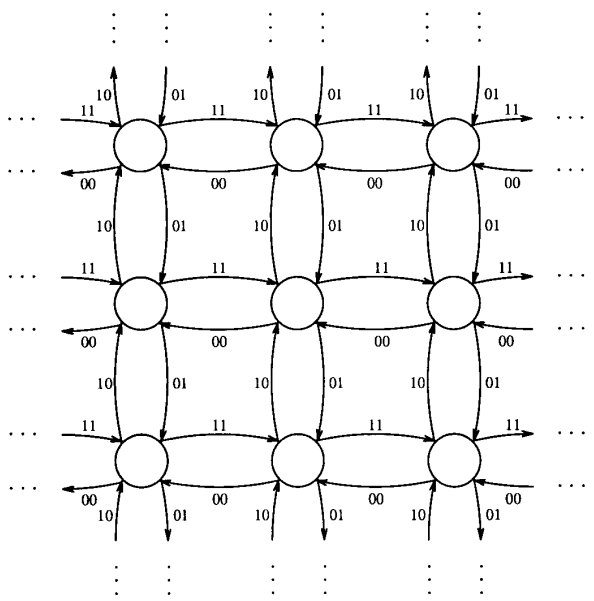


Fig. 1. Cross-product of two canonical diagrams of single-track MSN codes G.

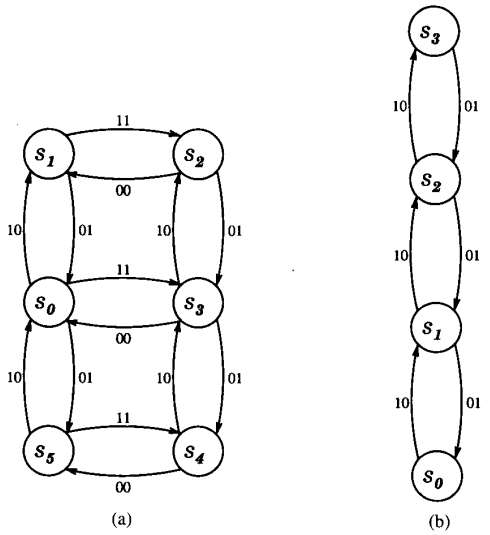
Note that

$$\|\overline{e}_l\|_X^2 = \overline{e}_l X \overline{e}_l' = \|e_l(D)F(D)\|^2$$

where X and $F(D)$ are as previously defined and the squared norm of a polynomial refers to the sum of its squared coefficients.

Let G be the graph representing the cross-product of two canonical diagrams of single-track MSN codes, shown in Fig. 1, and the recorded two-track sequences be given by $a_{nl} = 2u_{nl} - 1, l = 1, 2$. Then $\boldsymbol{\epsilon}$ of (10) is the normalized error sequence defined earlier, and $\|\overline{e}_l\|_X^2 \ge d_0^2 = 2, l = 1, 2$. From the proof of Proposition 1, we see that the worst case error events (those for which $d_{\min}^2$ is achieved) in the range of ITI for which the additional loss in performance occurs are those for which $\overline{e}_1 = -\overline{e}_2$ and $\|\overline{e}_1\|_X^2 = \|\overline{e}_2\|_X^2 = d_0^2$. To eliminate these error events, we need to impose a constraint that would guarantee that $\overline{e}_1 = -\overline{e}_2$ implies $\|\overline{e}_1\|_X^2 = \|\overline{e}_2\|_X^2 > d_0^2$. Therefore, our goal is to limit the set of possible sequences $\boldsymbol{u}$ by removing some edges of G so that for all difference cycles, $\overline{e}_1 = -\overline{e}_2$ implies $\|\overline{e}_1\|_X^2 = \|\overline{e}_2\|_X^2 \ge 3$. The remaining subgraph should not have subgraphs of the forms shown in Fig. 2. For the graph of Fig. 2(a), let $\boldsymbol{u}$ be the sequence generated by path $\{s_0, s_1, s_2, s_3, s_0\}$ and $\boldsymbol{v}$ be the sequence generated by path $\{s_0, s_5, s_4, s_3, s_0\}$. Then for the difference cycle corresponding to $\boldsymbol{u}$ and $\boldsymbol{v}$, we have $\overline{e}_1 = -\overline{e}_2$ and $\|\overline{e}_1\|_X^2 = \|\overline{e}_2\|_X^2 = 2$. For the graph of Fig. 2(b), let $\boldsymbol{u}$ be the sequence generated by path $\{s_1, s_2, s_3, s_2, s_1\}$ and $\boldsymbol{v}$ be the sequence generated by path $\{s_1, s_0, s_1, s_0, s_1, \}$. Then for the difference cycle corresponding to $\boldsymbol{u}$ and $\boldsymbol{v}$, we have $\overline{e}_1 = -\overline{e}_2$ and $\|\overline{e}_1\|_X^2 = \|\overline{e}_2\|_X^2 = 2$.

A subgraph of G that does not have subgraphs of the above discussed forms is shown in Fig. 3 and is denoted by G_N. In the set of nodes of G_N, we distinguish two boundary nodes



(a) (b)

Fig. 2. FSTD's to be excluded from G.

s and t and the nodes that form the main body of the graph. These nodes are grouped in three classes: σ with four outgoing edges, κ with two outgoing edges, and τ with one outgoing edge. The number of nodes in each class, $N+1$, is chosen according to the target code rate. We first consider distance properties of the set of sequences represented by G_N, and then construct several high-rate codes based on G_N for various N.

Proposition 2: Let G_N be the irreducible FSTD in Fig. 3 and

$$\{x_k\} \stackrel{\text{DFT}}{\longleftrightarrow} X(D) = F(D)F^*(D^{-1}), \quad F(D) = (1-D)/\sqrt{2}. \tag{11}$$

Let $\boldsymbol{u} = \overline{u}_0, \cdots, \overline{u}_n$ and $\boldsymbol{v} = \overline{v}_0, \cdots, \overline{v}_n$ be two distinct sequences, with $\overline{u}_0 \neq \overline{v}_0$, generated by two paths in $G_N, \Sigma_u = \{s_0, s_1^u, \cdots, s_n^u, s_0\}$ and $\Sigma_v = \{s_0, s_1^v, \cdots, s_n^v, s_0\}$. Let $\overline{e}_1$ and $\overline{e}_2$ be difference cycles corresponding to $\boldsymbol{u}$ and $\boldsymbol{v}$ on tracks 1 and 2, respectively. Then $\overline{e}_1 = -\overline{e}_2$ implies $\|\overline{e}_1\|_X^2 = \|\overline{e}_2\|_X^2 \geq 3$.

Proof of Proposition 2: From the structure of G_N and $\overline{u}_0 \neq \overline{v}_0$, we conclude that $\overline{e}_1 = -\overline{e}_2 \neq \overline{0}$ requires that

1) s_0 be one of the σ-states, i.e., $s_0 = \sigma_i$ for some $i, 0 \leq i \leq N$, and $s_1^v = \tau_i$ and $s_1^u = \kappa_i$ or *vice versa*;
2) paths Σ_u and Σ_v either stay on the subgraph of G_N defined by states $\kappa_i, \sigma_i, \tau_i$ (shown in the dotted box in the figure) or both depart from it at state σ_i at the same time, $m, 2 \leq m \leq n-1$, to the same state κ_{i-1} or κ_{i+1}.

Note that G_N is a subgraph of the graph representing the cross-product of two canonical diagrams for single-track MSN codes [13]. Therefore, $\|\overline{e}_l\|_X^2 \geq 2$, and, when $\overline{u}_l$ and $\overline{v}_l$ are entirely on the subgraph $\kappa_i, \sigma_i, \tau_i$, then $\|\overline{e}_l\|_X^2 \geq 3$ (recall that the binary biphase code provides an increase of 4.8 dB in the single-track minimum distance). From requirements 1 and 2 we conclude that difference cycle $\overline{e}_l = e_{0l}, \cdots, e_{nl}$ consists of two concatenated difference cycles

$$\overline{e}_l^1 = e_{0l}^1, \cdots, e_{(m-1)l}^1 = e_{0l}, \cdots, e_{(m-1)l}$$

and

$$\overline{e}_l^2 = e_{0l}^2, \cdots, e_{(n-m)l}^2 = e_{ml}, \cdots, e_{nl}.$$

Thus $e_l(D) = e_l^1(D) + D^m e_l^2(D)$, where the degree of $e_l^1(D)$ is at most $(m-1)$. From requirement 2 we conclude that $e_{ml} = e_{0l}^2 = 0$. Since the difference cycle $\overline{e}_l^1$ corresponds to the parts of Σ_u and Σ_1 that are entirely on the subgraph $\kappa_i, \sigma_i, \tau_i, \|e_l^1(D)(1-D)\|^2/2 \geq 3$. Therefore

$$\begin{aligned}\|e_l(D)F(D)\|^2 &= \|(e_l^1(D) + D^m e_l^2(D))(1-D)\|^2/2 \\ &= \|e_l^1(D)(1-D) + D^m e_l^2(D)(1-D)\|^2/2 \\ &= \|e_l^1(D)(1-D)\|^2/2 \\ &\quad + \|e_l^2(D)(1-D)\|^2/2 \\ &\geq 3\end{aligned}$$

which completes the proof. Equality above is achieved, for example, when $\Sigma_u = \{\sigma_i, \kappa_i, \sigma_i\}$ and $\Sigma_v = \{\sigma_i, \tau_i, \sigma_i\}$ in which case $\overline{e}_1 = -\overline{e}_2$ and $\|\overline{e}_1\|_X^2 = \|\overline{e}_2\|_X^2 = 3$. ■

Note that Proposition 2 may be satisfied for some other subgraphs of the cross-product of two canonical diagrams for single-track MSN codes, not necessarily of G_N type, but G_N (actually the irreducible component of the second power of G_N that consists only of the σ-states) has some attractive symmetry properties, useful for computing capacity and designing finite-state encoders with sliding-block decoders.

Proposition 3: Let $G_N, \boldsymbol{u}, \boldsymbol{v}$, and x_k be as previously defined. Then

$$d_{\min}^2 = \begin{cases} 2(1+\alpha^2), & \text{if } 0 \leq \alpha \leq (3-\sqrt{5})/2 \\ 6(1-\alpha)^2, & \text{if } (3-\sqrt{5})/2 \leq \alpha \leq 1/2. \end{cases} \tag{12}$$

Proof of Proposition 3: Since G_N is a subgraph of the graph representing the cross-product of two canonical diagrams of single-track MSN codes, the single-track minimum distances satisfy $\|\overline{e}_1\|_X^2 \geq 2$ and $\|\overline{e}_2\|_X^2 \geq 2$. From (6)

$$\begin{aligned}d^2(\boldsymbol{\epsilon}) &= (1+\alpha^2)(\|\overline{e}_1\|_X^2 + \|\overline{e}_2\|_X^2) + 2 \cdot 2\alpha\langle\overline{e}_1, \overline{e}_2\rangle_X \\ &\geq (1+\alpha^2)(\|\overline{e}_1\|_X^2 + \|\overline{e}_2\|_X^2) - 2\alpha \cdot 2|\langle\overline{e}_1, \overline{e}_2\rangle_X|.\end{aligned}$$

Moreover, from $\|\overline{e}_1 \pm \overline{e}_2\| \geq 0$

$$2|\langle\overline{e}_1, \overline{e}_2\rangle_X| \leq \|\overline{e}_1\|_X^2 + \|\overline{e}_2\|_X^2 \tag{13}$$

with equality iff $\overline{e}_1 = \pm\overline{e}_2$, and from (11), $2|\langle\overline{e}_1, \overline{e}_2\rangle_X|$ is an integer. We distinguish the following possibilities regarding error sequences $\boldsymbol{\epsilon}$:

1) Errors occur in only one track, in which case either $\overline{e}_1 = \overline{0}$ or $\overline{e}_2 = \overline{0}$. Then

$$\langle\overline{e}_1, \overline{e}_2\rangle_X = 0, (\|\overline{e}_1\|_X^2 + \|\overline{e}_2\|_X^2) \geq 2$$

and thus

$$d^2(\boldsymbol{\epsilon}) \geq 2(1+\alpha^2).$$

2) Errors occur in both tracks, in which case $\overline{e}_1 \neq \overline{0}$ and $\overline{e}_2 \neq \overline{0}$. We have the following further partition:
   a) $\overline{e}_1 \neq \pm\overline{e}_2$. In this case (since $2|\langle\overline{e}_1, \overline{e}_2\rangle_X|$ is an integer and the necessary and sufficient condition for equality in (13) does not hold)

$$2|\langle\overline{e}_1, \overline{e}_2\rangle_X| \leq \|\overline{e}_1\|_X^2 + \|\overline{e}_2\|_X^2 - 1$$

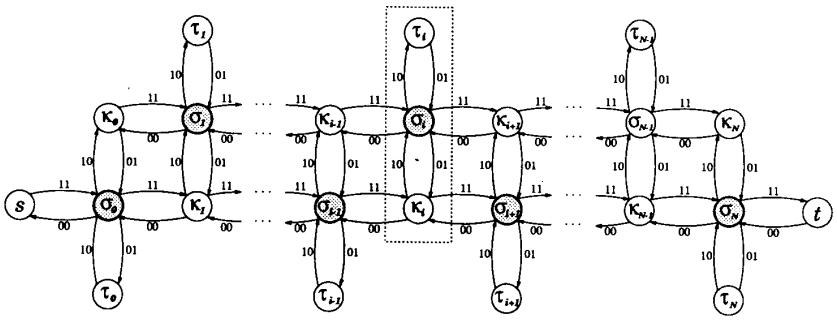


Fig. 3. G_N.

and thus

$$\begin{aligned} d^2(\epsilon) &\geq (1+\alpha^2)(\|\bar{e}_1\|_X^2 + \|\bar{e}_2\|_X^2) - 2\alpha \cdot 2|\langle \bar{e}_1, \bar{e}_2 \rangle_X| \\ &\geq (1+\alpha^2)(\|\bar{e}_1\|_X^2 + \|\bar{e}_2\|_X^2) \\ &\quad - 2\alpha(\|\bar{e}_1\|_X^2 + \|\bar{e}_2\|_X^2 - 1) \\ &= (1-\alpha)^2(\|\bar{e}_1\|_X^2 + \|\bar{e}_2\|_X^2) + 2\alpha \\ &\geq 4(1-\alpha)^2 + 2\alpha. \end{aligned}$$

b) $\bar{e}_1 = \bar{e}_2$. In this case

$$\begin{aligned} d^2(\epsilon) &= 2(1+\alpha)^2\|\bar{e}_1\|_X^2 \\ &\geq 4(1+\alpha)^2. \end{aligned}$$

c) $\bar{e}_1 = -\bar{e}_2$. We have

$$\begin{aligned} d^2(\epsilon) &= 2(1+\alpha^2)\|\bar{e}_1\|_X^2 - 4\alpha\|\bar{e}_1\|_X^2 \\ &= 2(1-\alpha)^2\|\bar{e}_1\|_X^2 \\ &\geq 6(1-\alpha)^2 \end{aligned}$$

where the last bound follows from Proposition 2. Taking the minimum of $d^2(\epsilon)$ with respect to α we obtain (12) for $0 \leq \alpha \leq 1/2$. ■

Results of Propositions 1 and 3 and Corollary 1 are summarized in Fig. 4, which shows the two-track minimum distance parameter for an uncoded and three-coded systems. Coded system 1 applies a two-track code constructed from G_N at a rate up to its capacity (which depending on N is between 1/2 and 0.8305 ... as we will see later), and provides an increase in minimum distance of 3 dB (compared to the uncoded system) for interference levels of $0 \leq \alpha \leq 2-\sqrt{3}$, $20\log_{10}[(1+\alpha)/(1-\alpha)]$ dB for $2-\sqrt{3} \leq \alpha \leq 1-\sqrt{3}/3$, and 4.8 dB for $1-\sqrt{3}/3 \leq \alpha \leq 1/2$. Coded system 2 applies the rate 1/2 biphase code on each of the two tracks, and provides an increase in minimum distance of 4.8 dB for interference levels of $0 \leq \alpha \leq 1/2$. Coded system 3 applies a single-track MSN code of rate higher than 1/2 on each of the tracks, and provides an increase in minimum distance of 3 dB for interference levels of $0 \leq \alpha \leq 1/2$.

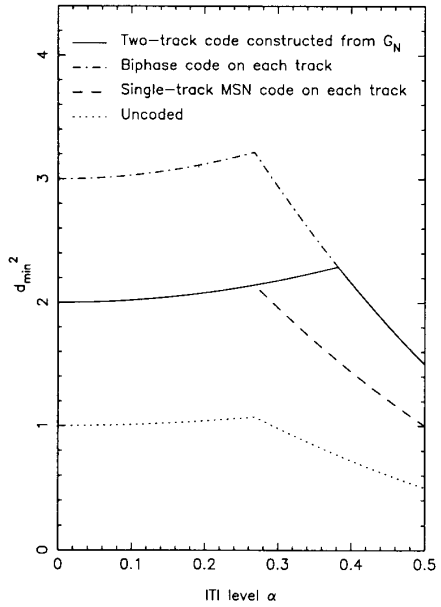


Fig. 4. Performance of the optimal two-head detector for a channel of two interfering tracks with and without coding.

C. High-Rate Codes Constructed from G_N

Design and demodulation issues for codes constructed from G_N are addressed in the same manner as for the single-track MSN codes [13]. Since G_N is of almost finite type (AFT), there exists a finite-state encoder with a sliding-block decoder at any rate below the Shannon capacity of G_N, but there is no systematic code construction algorithm [14] for obtaining such encoders. We consider codes for which the encoder and the reduced-complexity detector trellis are constructed from G_N^σ, the irreducible component of the second power of G_N that consists only of the σ-states. This component, as previously mentioned, has some symmetry properties useful for computation of the capacity and design of finite-state encoders with sliding-block decoders. The adjacency matrix of G_N^σ is given by

$$B_N = \begin{bmatrix} 4 & 2 & 1 & 0 & \cdots & 0 & 0 \\ 2 & 4 & 2 & 1 & \cdots & 0 & 0 \\ 1 & 2 & 4 & 2 & \cdots & 0 & 0 \\ \vdots & \vdots & \vdots & \vdots & & \vdots & \vdots \\ 0 & 0 & 0 & 0 & \cdots & 4 & 2 \\ 0 & 0 & 0 & 0 & \cdots & 2 & 4 \end{bmatrix}_{(N+1)\times(N+1)}$$

The Shannon capacity of G_N^σ, denoted by C_N^σ, is equal to

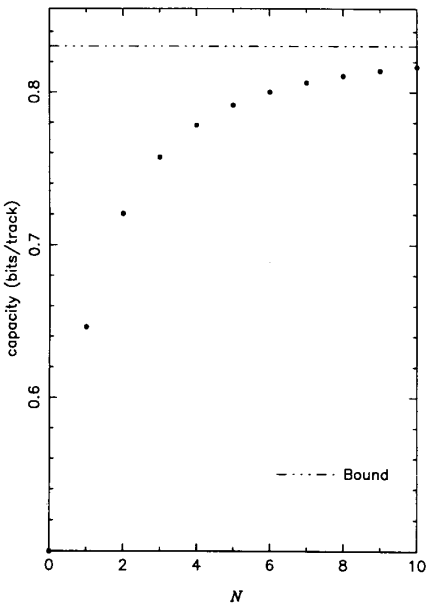


Fig. 5. The capacity of G_N as a function of N.

$\log \lambda_{\max}^N$, where $\lambda_{\max}^N$ is the maximum eigenvalue of B_N. An upper bound on $\lambda_{\max}^N$ can be found simply by applying Geršgorin's theorem (see, for example, [15]) or the well-known results on Toeplitz matrices [16]

$$\lambda_{\max}^N \leq 4 + 1 + 2 + 2 + 1 = 10.$$

Since each branch of G_N^σ is actually two branches of G_N and each branch of G_N carries 2 bits for two tracks, the Shannon capacity of G_N *per track*, denoted by C_N, is equal to $C_N^\sigma/4$. The rates per track of the codes that can be constructed from G_N^σ are therefore limited by

$$C_N = \tfrac{1}{4} \log \lambda_{\max}^N \leq \tfrac{1}{4} \log_2 10 = 0.8305 \cdots.$$

A rate 2/3 code can be constructed from G_2^σ, a rate 3/4 from G_3^σ, and a rate 4/5 from G_7^σ. The capacity of G_N as a function of N, together with the above bound, is shown in Fig. 5.

We constructed and tested by computer-simulation codes of rates 5/8 and 8/12 from G_2^σ, and 3/4 from G_5^σ (the irreducible component of the second power of a modified version of G_5 that consists only of the σ-states, shown in Fig. 6). Construction of encoders with sliding-block decoders for 5/8 and 8/12 rate codes from G_2^σ was a straightforward application of the splitting algorithm of Adler, Coppersmith and Hassner [17] (see also Marcus, Siegel, and Wolf [18] for an excellent tutorial exposition on the topic). The rate 5/8 code has a 4-state encoder graph, an 8-state reduced-complexity Viterbi detector, and a sliding-block decoder with one codeword look-ahead. The maximum length of an error burst in the decoded data sequence resulting from a single error in the detected data sequence is thus limited to 10 bits. The run-lengths of symbols $(1,1)$ and $(0,0)$ are limited to 2. The rate 8/12 code has a 4-state encoder graph, a 10-state reduced-complexity Viterbi detector, and a sliding-block decoder with one codeword look-ahead. The maximum length of an error burst in the decoded data sequence resulting from a single error in the detected data sequence is thus limited to 16 bits. The run-lengths of symbols $(1,1)$ and $(0,0)$ are limited to 3. Computer-simulated performance results for both codes at various ITI levels show excellent agreement with the predicted performance addressed in the previous subsection, i.e., for high SNR, the probability of error is about $Q(d_{\min}\sqrt{\text{SNR}})$ where $d_{\min}^2$, as a function of ITI, is given in Fig. 4.

TABLE I
ENCODER FOR RATE 3/4 CODE

	Current state									
Input	s_0	s_1	s_2	s_3	s_4	s_5	s_6	s_7	s_8	s_9
000	11/s_2 11/s_3	11/s_3 11/s_3	00/s_0 00/s_0	00/s_1 00/s_1	00/s_2 00/s_2	00/s_3 00/s_3	11/s_1 00/s_1	11/s_2 00/s_2	11/s_3 00/s_3	11/s_4 00/s_4
001	11/s_7 11/s_7	11/s_8 11/s_8	11/s_9 11/s_9	00/s_6 00/s_6	00/s_7 00/s_7	00/s_8 00/s_8	11/s_6 00/s_6	11/s_7 00/s_7	11/s_8 00/s_8	11/s_9 00/s_9
010	10/s_0 01/s_0	10/s_1 01/s_1	10/s_2 01/s_2	10/s_3 01/s_3	10/s_4 01/s_4	10/s_5 01/s_5	00/s_1 11/s_1	00/s_2 11/s_2	00/s_3 11/s_3	00/s_4 11/s_4
011	11/s_6 10/s_6	10/s_6 01/s_6	10/s_7 01/s_7	10/s_8 01/s_8	10/s_9 01/s_9	01/s_9 00/s_9	00/s_6 11/s_6	00/s_7 11/s_7	00/s_8 11/s_8	00/s_9 11/s_9
100	10/s_1 11/s_1	01/s_6 10/s_6	01/s_7 10/s_7	01/s_8 10/s_8	01/s_9 10/s_9	00/s_9 01/s_9	01/s_2 11/s_2	00/s_1 10/s_1	01/s_4 11/s_4	00/s_2 10/s_2
101	01/s_0 10/s_0	01/s_1 10/s_1	01/s_2 10/s_2	01/s_3 10/s_3	01/s_4 10/s_4	01/s_5 10/s_5	01/s_7 11/s_7	00/s_6 10/s_6	01/s_9 11/s_9	00/s_8 10/s_8
110	10/s_1 11/s_1	00/s_0 01/s_0	10/s_3 11/s_3	00/s_2 01/s_2	10/s_5 11/s_5	00/s_4 01/s_4	11/s_2 01/s_2	10/s_1 00/s_1	11/s_4 01/s_4	10/s_3 00/s_3
111	11/s_1 10/s_1	01/s_0 00/s_0	11/s_3 10/s_3	01/s_2 00/s_2	11/s_5 10/s_5	01/s_4 00/s_4	11/s_7 01/s_7	10/s_6 00/s_6	11/s_9 01/s_9	10/s_8 00/s_8

Construction of an encoder with a sliding-block decoder for a rate 3/4 code from G_5^σ required some craftiness [12], [19]. Tables I and II present the resulting encoder and sliding-block decoder, Fig. 7 the reduced-complexity detector trellis, and Fig. 8 shows computer-simulated performance results for this code. The encoder was constructed from G_5^σ by splitting states $\sigma_1, \sigma_2, \sigma_3$, and σ_4 in one round of splitting. The states are split, unnecessary branches deleted, and input tags are assigned such that the resulting encoder has a sliding-block decoder requiring one codeword look-ahead and producing run-lengths of symbols $(1,1)$ and $(0,0)$ limited to 5. The 10-state encoder is described by Table I. The states are denoted by $s_0, \cdots, s_9$, and the input words are the binary 3-tuples $\boldsymbol{b} = b_1 b_2 b_3$. For a given state and input, the output is a two-column codeword $\boldsymbol{c}$ with a next state $t \in \{s_0, \cdots, s_9\}$. The two columns corresponding to the two tracks contain 2 bits each. The table entry in column s_i and row $\boldsymbol{b}$ is the output and the next state in the form $\boldsymbol{c}/t$.

The sliding-block decoder requiring one codeword look-ahead is described in Table II. The maximum length of an error burst in the decoded data sequence resulting from a single error in the detected data sequence is limited to 6 bits.

The reduced-complexity detector trellis for this code for the two-track, dicode channel is based upon G_5^σ, and is shown in Fig. 7. The trellis is constructed in the same manner as in single-track MSN codes for $(1-D)$ channel [13]. A state in the trellis ρ is defined by $\boldsymbol{a}$, a binary pair of symbols corresponding to the two tracks, and σ_i, a state in $G_5^\sigma, 0 \leq i \leq 5$. For a state $\rho = (\boldsymbol{a}, \sigma_i)$, the set of all possible inputs and corresponding transitions is determined only by σ_i. Therefore, for the sake of clarity, these sets are shown in Fig. 7 only once for each group of states having the same σ_i.

Computer-simulated performance results for four different ITI levels, together with a lower bound to the probability of error of the normalized uncoded $(1 - D)$ channel,

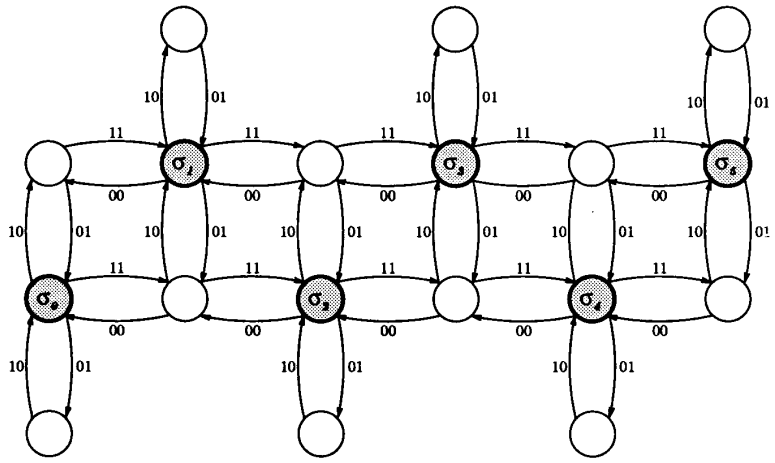


Fig. 6. G_5^q.

TABLE II
SLIDING-BLOCK DECODER FOR RATE 3/4 CODE.

Current Codeword	Next Codeword	
	00 00 01 01 10 10 11 11 00 01 00 10 01 11 10 11	00 00 01 10 11 11 10 11 11 00 00 01
00 00	000	001
00 01	110	100
00 10	100	101
00 11	010	011
01 00	111	011
01 10	101	100
01 11	100	101
10 00	110	111
10 01	010	011
10 11	110	100
11 00	000	001
11 01	110	111
11 10	111	011
11 11	000	111

$Q(1 \cdot \sqrt{\text{SNR}})$, are shown in Fig. 8. The analytically computed $d^2_{\min}$, shown in Fig. 4, has been verified by the performance gains obtained for high SNR, for which the probability of error is closely approximated by $Q(d_{\min}\sqrt{\text{SNR}})$. The performance of this code for $\alpha = 0$ matches the performance of the rate 3/4 MSN code for the single-track case, as presented in [13].

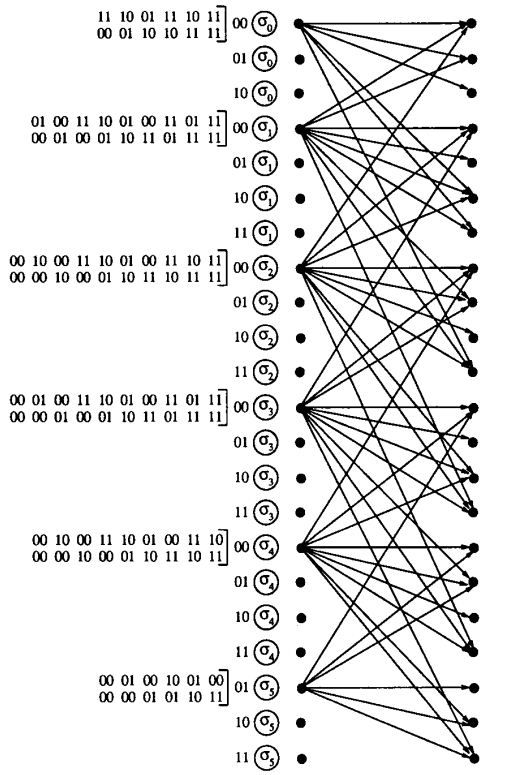


Fig. 7. Reduced-complexity Viterbi detector trellis for the rate 3/4 code. For clarity, not all branches are shown.

IV. CONCLUSIONS

We have shown that multidimensional modulation codes combined with simultaneous reading of multiple tracks can more than compensate for the performance loss incurred by track-narrowing over a wide range of ITI levels. For the special case of the two-track, two-head, dicode channel, two-dimensional codes were designed capable of recovering the SNR loss incurred by ITI for large interference levels. Sliding-block decoders and reduced-complexity Viterbi detectors were also obtained for the designed codes.

The codes discussed here were derived for a special model of interference that exists between tracks assuming there is no servo positioning error [4], [20]. However, the codes are expected to be applicable in systems with known and unknown servo positioning errors as well.

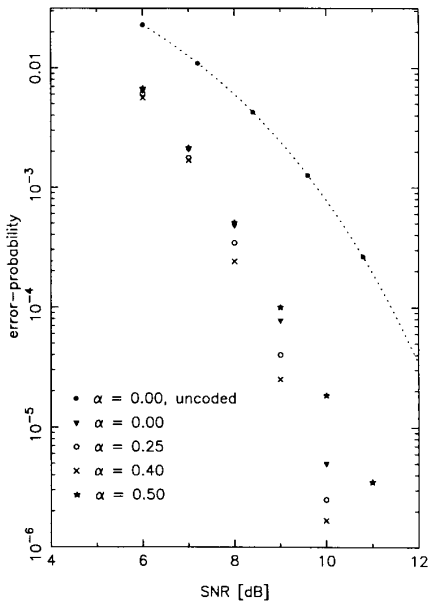


Fig. 8. Performance of rate 3/4 two-track code for four different interference levels.

REFERENCES

[1] P. H. Siegel and J. K. Wolf, "Modulation and coding for information storage," *IEEE Commun. Mag.*, vol. 29, no. 12, pp. 68–86, Dec. 1991.

[2] L. C. Barbosa, "A simultaneous maximum likelihood estimation of sequences for interfering synchronous channels," IBM Res. Rep. RJ-5625.

[3] ——, "Maximum likelihood sequence estimators: A geometric view," *IEEE Trans. Inform. Theory*, vol. 35, no. 2, pp. 419–427, Mar. 1989.

[4] ——, "Simultaneous detection of readback signals from interfering magnetic recording tracks using array heads," *IEEE Trans. Magn.*, vol. 26, no. 5, pp. 2163–2165, Sept. 1990.

[5] W. L. Abbot, J. M. Cioffi, and H. K. Thapar, "Performance of digital magnetic recording with equalization and off-track interference," *IEEE Trans. Magn.*, vol. 27, no. 1, pp. 705–716, Jan. 1991.

[6] P. A. Voois and J. M. Cioffi, "A decision feedback equalizer for multiple-head digital magnetic recording," in *Proc. 1991 IEEE Int. Conf. on Communications (ICC '91)* (Denver, CO, June 1991), pp. 26.4.1–26.4.5.

[7] ——, "Multichannel digital magnetic recording," in *Proc. 1992 IEEE Int. Conf. on Communications (ICC '92)* (Chicago, IL, June 1992), pp. 305.4.1–205.4.6.

[8] ——, "Achievable radial information densities in magnetic recording systems," in *Proc. 1992 IEEE Global Telecommunications Conf. (GLOBECOM '92)* (Orlando, FL, Dec. 1992), pp. 1067–1071.

[9] M. W. Marcellin and H. J. Weber, "Two-dimensional modulation codes," *IEEE J. Selected Areas Commun.*, vol. 10, no. 1, pp. 254–266, Jan. 1992.

[10] R. E. Swanson and J. K. Wolf, "A new class of two-dimensional RLL recording codes," *IEEE Trans. Magn.*, vol. 28, no. 6, pp. 3407–3416, Nov. 1992.

[11] E. Soljanin and C. N. Georghiades, "On coding in multi-track, multi-head, disk recording systems," in *Proc. 1993 IEEE Global Telecommunications Conf. (GLOBECOM '93)* (Houston, TX, Nov. 1993), pp. 18–22.

[12] E. Soljanin "Coding for improving noise immunity in multi-track, multi-head recording systems," Ph.D. dissertation, Texas A&M Univ., College Station, TX, Aug. 1994.

[13] R. Karabed and P. H. Siegel, "Matched spectral-null codes for partial response channels," *IEEE Trans. Inform. Theory*, vol. 37, no. 3, pt. II, pp. 818–855, May 1991.

[14] R. Karabed and B. H. Marcus, "Sliding-block coding for input-restricted channels," *IEEE Trans. Inform. Theory*, vol. 34, no. 1, pp. 2–26, Jan. 1988.

[15] P. Lancaster and M. Tismentsky, *The Theory of Matrices*. San Diego, CA: Academic Press, 1985.

[16] U. Grenander and G. Szegö, *Toeplitz Forms and Their Applications*. Berkeley, CA: Univ. of Calif. Press, 1958.

[17] R. Adler, D. Coppersmith, and M. Hassner, "Algorithms for sliding-block codes," *IEEE Trans. Inform. Theory*, vol. IT-29, no. 1, pp. 5–22, Jan. 1983.

[18] B. H. Marcus, P. H. Siegel, and J. K. Wolf, "Finite-state modulation codes for data storage," *IEEE J. Selected Areas Commun.*, vol. 10, no. 1, pp. 5–37, Jan. 1992.

[19] E. Soljanin and C. N. Georghiades, "Sliding-block codes for two-track magnetic recording channels," in *Proc. 28th Annual Conf. om Information Sciences and Systems (CISS '94)* (Princeton, NJ, Mar. 1994), pp. 1–5.

[20] M. P. Vea and J. M. F. Moura, "Magnetic recording channel model with intertrack interference," *IEEE Trans. Magn.*, vol. 27, no. 6, pp. 4834–4836, Nov. 1991.